Geomicrobiology Journal
Publication details, including instructions for authors and subscription information:
http://www.tandfonline.com/loi/ugmb20

Assessment of the Resistance to Uranium (VI) Exposure by Arthrobacter sp. Isolated from Hanford Site Soil

Yelena Katsenovich [a], Denny Carvajal [a], Rakesh Guduru [a b], Leonel Lagos [a] & Chen-Zhong Li [b]

[a] Applied Research Center, Florida International University, Miami, Florida, USA
[b] Nanobioengineering/Bioelectronic Lab, Department of Biomedical Engineering, Florida International University, Miami, Florida, USA

Accepted author version posted online: 06 Jun 2012.Version of record first published: 07 Dec 2012.

To cite this article: Yelena Katsenovich , Denny Carvajal , Rakesh Guduru , Leonel Lagos & Chen-Zhong Li (2013): Assessment of the Resistance to Uranium (VI) Exposure by Arthrobacter sp. Isolated from Hanford Site Soil, Geomicrobiology Journal, 30:2, 120-130

To link to this article: http://dx.doi.org/10.1080/01490451.2011.654376

Geomicrobiology Journal (2013) **30**, 120–130

ISSN: 0149-0451 print / 1521-0529 online
DOI: 10.1080/01490451.2011.654376

Taylor & Francis
Taylor & Francis Group

Assessment of the Resistance to Uranium (VI) Exposure by *Arthrobacter* sp. Isolated from Hanford Site Soil

YELENA KATSENOVICH[1]*, DENNY CARVAJAL[1], RAKESH GUDURU[1,2], LEONEL LAGOS[1], and CHEN-ZHONG LI[2]

[1]*Applied Research Center, Florida International University, Miami, Florida, USA*
[2]*Nanobioengineering/Bioelectronic Lab, Department of Biomedical Engineering, Florida International University, Miami, Florida, USA*

Received February 2011, Accepted December 2011

Production of nuclear fuel has resulted in hazardous waste streams that have contaminated the soil and groundwater. *Arthrobacter* strains, G975, G968, and G954 were used in the prescreening tests to evaluate their tolerance to UO_2^{2+} and investigate bacteria-U(VI) interactions under oxidizing pH-neutral conditions. Experiments have shown G975 is the fastest growing and the most uranium tolerant strain that removed about 90% of uranium from growth media. Atomic Force Microscopy images exhibited an irregular surface structure, which perhaps provided a larger surface area for uranium precipitation. The data indicate that aerobic heterotrophic bacteria may offer a solution to sequestering uranium in oxic conditions, which prevail in the vadose zone.

Keywords: *Arthrobacter* strains, viability, resistance, radionuclides, microscopy

Introduction

Production of nuclear fuel at Hanford Site, Washington has resulted in a wide variety of hazardous waste streams composed of chemical and radiological constituents. Despite extensive remediation efforts, persistent groundwater plumes containing uranium concentrations exceeding 30 ppb, the U.S. Environmental Protection Agency (EPA) standard for drinking water supplies, have formed in multiple locations at Hanford. There is concern that elevated uranium concentrations could enter the Columbia River along the shoreline contaminating sediment and aquatic biota (Zachara et al. 2007).

Uranium (VI) is the most stable valence of uranium under oxidizing conditions, and due to complicated chemical behavior, it readily forms complexes with a variety of ligands (Grenthe et al. 2004). Common ligands in the environment that form stable uranyl solid phases include: hydroxyl, phosphate, carbonate, silicate and organic substances (Burns 1999; Davis 2001; Lenhart et al. 2000). These complexation reactions often result in the formation of mobile aqueous species or precipitation of U-bearing minerals (Finch and Murakami 1999). The migration of U(VI) in the Hanford subsurface is retarded by both complexation to mineral surfaces and precipitation with the formation of U-containing mineral phases such as silicates and phosphates (Zachara et al. 2007).

Data reported in literature suggests that indigenous microorganisms in subsurface environments play a major role in a mineral weathering process and can affect the mobility of heavy metals or radionuclides by dissolution, complexation reactions due to the secretion of protons and various ligands, and physico-chemical interactions between the uranyl cation and the bacterial cell wall polymers (Fredrickson et al. 2004; Suzuki and Banfield 2004). These can result in a decrease of long-term stability of precipitated U(VI).

Of considerable interest to our investigation was aerobic, Gram-positive *Arthrobacter* sp., which comprises a very diverse group known for their ability to survive in extreme conditions. *Arthrobacter* bacteria are one of the most numerous groups in soils and were found in fairly large numbers in contaminated Hanford vadose zone soil and various other subsurface environments contaminated with heavy metals and radioactive materials (Balkwill et al. 1997; Boylen 1973; Mongodin et al. 2006; Van Waasbergen et al. 2000). Previous studies have revealed that this genus plays a significant role in natural environments and, in addition, well adapted

Funding for this research was provided by US DOE Grant Number: DE-FG01-05EW07033. We would like to thank Dr. David Balkwill for providing us with *Arthrobacter* sp. strains and acknowledge Dr. Yanqing Liu from the FIU Advanced Materials Engineering Research Institute (AMERI) for his assistance with the SEM images and EDS analysis of bacterial surface composition. We are grateful to Dr. Mathew Marshall of Pacific Northwest National Laboratory (PNNL) for reviewing the manuscript and providing valuable comments and suggestions. We thank two anonymous reviewers for their positive and constructive comments.

*Address correspondence to Yelena Katsenovich, Applied Research Center, Florida International University, 10555 W. Flagler Street, Miami, FL 33174, USA; Email: katsenov@fiu.edu

to nutrient-deprived (oligotrophic) conditions (Crocker et al. 2000; Kieft 2002; Osman et al. 2008).

Boylen (1973) assessed the ability of *A. crystallopoietes* to survive extended periods of drought and determined that under the experimental conditions, both morphological forms of *Arthrobacter* were equally resistant to desiccation.

Arthrobacter can survive in extreme conditions associated with UV-irradiation and radioactivity (Osman et al. 2008). Microorganisms with the closest match to a member of the genus *Arthrobacter* were the most prevalent in the highly radioactive sediment samples collected underneath the leaking radionuclide storage tanks and accounted for about one-third of the total soil isolatable bacterial population (Fredrickson et al. 2004).

Bacterial resistance to heavy metals is ecologically important. *Arthrobacter* have developed very efficient molecular adaptation mechanisms that enhance the stability of nucleic acids, proteins, and lipids allowing bacteria to survive in stressful conditions (Mongodin et al. 2006).

Physical and chemical interactions involving adsorption, ion exchange, and complexation are driven forces of extracellular association of uranium with bacterial cell surfaces, which does not depend on metabolism. Bacterial cell walls, proteins, and lipids contain functional groups such as carboxyl and phosphate, which are able to bind with uranium (Francis 2008). The results of EXAFS analysis of the association of U with bacterial cells showed that it was associated predominantly with phosphate in the form of uranyl phosphate, and with other ligands such as the carboxyl species (Beazley et al. 2007; Francis et al. 2004). In addition, *Arthrobacter* sp. can sequester uranium intracellularly in precipitates closely associated with polyphosphate granules. This phenomenon is associated with cell metabolism and possibly involves transport of metals across the cell membrane, which can be mediated by the mechanism used to convey metabolically essential ions such as sodium and potassium (Francis 2008).

The abundance of *Arthrobacter* sp. in bacterial populations of the actinide-contaminated Hanford Site sediments and their relatively high resistance to the toxic form of U(VI), determined the focus of this investigation on microorganisms of the genus *Arthrobacter*. Thus, the objective of this work was (i) to conduct prescreening tests with three heterotrophic Hanford Site isolates, (ii) investigate bacteria-U(VI) interactions under oxidizing pH-neutral conditions, and (iii) evaluate microbial growth and tolerance in the presence of the uranyl cation (UO_2^{2+}), which is a predominant U contaminant at Hanford Site (Zachara et al. 2007).

Materials and Methods

Growth Conditions of Arthrobacter *Strains*

Three *Arthrobacter* strains previously isolated from the Hanford subsurface were obtained from the Subsurface Microbial Culture Collection (SMCC) maintained in Florida State University, Tallahassee by Dr. Balkwill. Detailed descriptions of site geology, sample collection procedures, and methods of bacterial isolation are available from (Van Waasbergen et al. 2000). Identification of the *A. globiformis* (G954) and *A. oxydans* (G968, G975) strains was previously confirmed by 16S rDNA phylogeny (Balkwill et al. 1997; Van Waasbergen et al. 2000).

The strains were cultured in 5% PYTG medium consisting of 5 g/L peptone, 5 g/L tryptone, 10 g/L yeast extract, 10 g/L glucose, 0.6 g/L $MgSO_4.7H_2O$, 0.07 g/L $CaCl_2.2H_2O$ and 15 g/L agar. Media were prepared in deionized water (DIW), autoclaved at 121°C, 15 psi for 15 min, then the agar allowed to cool down to about 50° C before pouring into sterile petri dishes. To prevent any adverse effects on cell viability due to the decline in pH, liquid growth media were augmented with 1mM of 2-(2-hydroxyethyl)-1-piperazine ethanesulfonic acid sodium salt hydrate (HEPES-Na) buffer with pH adjusted to 7.0.

The *Arthrobacter* strains were aerobically grown to reach confluence in sterile foam stoppered 15 ml polypropylene centrifuge tubes amended with 3 mL of 5% PYTG media at 29°C in an incubator/shaker. All of the sets were inoculated with approximately 1.2E+06 cells of the corresponding strain to bring the final concentration of $\sim$ 4.E+05 cells/mL. Prior to inoculation, cell stock suspensions were vortexed for 10 seconds and counted using an INCYTO C-Chip disposable hemocytometer to calculate the amount of cell suspension needed to obtain the desired cell concentration in the tubes. After the tubes' inoculation, uranium was injected as uranyl nitrate from a stock solution of 0.005 M of U(VI) to achieve the desired concentration ranging between 0.5 ppm–57 ppm.

Abiotic controls composed of autoclaved PTYG media spiked with U(VI) were prepared for each target U(VI) concentration to account for possible losses due to interactions onto tubes walls, caps and complexation with the phosphorus-containing media components. Abiotic controls were assayed in the same way as experimental samples. To avoid the possibility of contamination from sampling of bacterial cultures, each set was prepared in triplicate and tubes were independently sampled at certain time intervals to obtain (i) cell counts using a hemocytometer, (ii) viable cell counts conducted by plating on sterile petri dishes, (iii) pH value, and (iv) the aqueous uranium concentrations.

Samples from each group (controls, incubated without uranium, and U(VI)-amended) were assayed at days 1, 2, 3, 6, and 7 by aseptically removing a representative sample. To account for viable bacteria, thoroughly mixed samples were subsequently diluted and homogeneous aliquots (0.1 mL) of the suspension from each dilution were uniformly spread on the sterile petri dishes. Viable microorganisms were calculated from the number of colony forming units (CFU) found on a specific dilution. In addition, the agar plating was used to provide a quick visual check for contamination and to maintain colonies from each stage of the enrichment for the duration of the experiment. The morphological details such as cell size, Gram stain reaction, and presence of a rod-coccus growth cycle were constantly monitored using an optical microscope. The morphological features recorded for colonies included presence of pigmentation, shape, type of edge, and type of surface.

The remaining solution was centrifuged for 5 min at the relative centrifugal force (RCF) of 3150 *g* and the supernatant was then analyzed for dissolved U(VI) with a Kinetic Phosphorescence Analyzer (KPA; Chemcheck Instruments,

Richland, WA). The same centrifugal force was used for all centrifugations. Uranium calibration standards (SPEX certiPrep), blanks and check standards (95–105% recovery) were analyzed for quality controls. Bioremoval of uranium was calculated against abiotic controls prepared with media solution amended with corresponding uranium concentrations and sampled at the same time intervals as experimental vials.

Total organic carbon (TOC) of centrifuged cell-free solutions was analyzed using a Shimadzu TOC analyzer with an autosampler (TOC-V CSH). Each analysis was repeated until the standard deviation was less than 3%. The pH values were measured using a pH microelectrode (Microelectrodes, Inc.). Equilibrium speciation modeling was conducted using Visual MINTEQ (v. 3.0, maintained by J.Gustafsson at KTH, Sweden, available at http://www.lwr.kth.se/English/OurSoftware/vminteq/ updated with the Nuclear Energy Agency's thermodynamic database for uranium [Guillaumont et al. 2003]). Testing on phosphorus (P) content in three PTYG media components such as yeast extract, peptone, and trypton, was conducted by EPA method 365.3. All experimental data was plotted and statistically analyzed using group comparison tests to identify two or more different sample groups for statistical significant differences through SigmaPlot for Windows Version 11.0.

Microscopy Techniques

The Meiji ML 2000 microscope was used for nondestructive examination of bacterial samples and quantification of cell densities by means of a hemocytometer (Fisher Scientific, Pittsburgh, PA). Cell counts in samples containing uranium employed INCYTO C-Chip disposable hemocytometers. Changes of the cell surface morphology were determined using a field emission scanning electron microscope (FE-SEM) and Energy-Dispersive Spectroscopy (EDS) analysis. Sample preparation procedures for SEM/EDS analysis included cells harvested by centrifugation for 5 min from PTYG media amended with a certain concentration of U(VI) and washing twice with a 50 mM of HEPES-Na prepared in DIW. The pH was adjusted to 7.2 with concentrated Fisher Scientific nitric acid (HNO_3).

The cells were fixed in the 5 ml of 2% glutaraldehyde in 0.1M HEPES-Na buffer at pH 7.2 for 2 h at 4°C. The fixative was changed at least twice. The material was removed by centrifugation and washed with 50 mM HEPES buffer 3 times for 10 min. The rinsed cells were then dehydrated in ethanol/water solutions of 35% (v/v), 70% (v/v), and 90% (v/v) each for 10 min, and twice in 100% (v/v) for 10 min.

Dehydrated samples were immersed for 10 min each in 50% and 100% pure hexamethyldisilazane (HMDS) (Pierce Biotechnology, Inc, Fisher Scientific) followed by 10 min of air-drying to allow liquid to evaporate from the samples (Araujo et al. 2003; Fratesi et al. 2004). The dehydrated specimens were then kept in the desiccators until time for the SEM/EDS assay. Treated and control samples were mounted on aluminum stubs with double sided sticky carbon tape and then coated for 30 sec with a thin layer of gold to increase conductivity. The microstructure of the gold-coated samples (Pelco SC-7, Auto sputter coater) was characterized using a JEOL, JSM-6330F SEM at 15 kV. The average cell surface composition was analyzed using a SEM-EDS Noran System Six Model 200.

The morphological and physiological changes of live bacterial cell surfaces at nanoscale spatial resolution were monitored using a MultimodeNanoscope IIIa atomic force microscopy (AFM) system from Veeco Instruments (Santa Barbara, California). High resolution phase imaging was performed by using Si_3N_4 soft tapping tips (BudgetSensors, Bulgaria) in order to ensure minimum sample damage with a constant force of 7.4 N/m and resonating frequency of 150 kHz. Phase imaging was performed in a TappingModeTM AFM to provide detailed information on the surface structure and its properties beyond the simple topography, which is not possible to achieve by any other microscopic technique. Sample preparation procedures included firm attachment of the bacterial cells onto the silicon wafer substrates ensuring cells were stable to the tip force. Bacterial samples were immobilized onto the 3-aminopropyltrimethoxysilane-coated silicon wafer substrates.

A 5–10 μl droplet of each concentrated bacterial suspension was placed onto a silanized silicon substrate. Excess water was then removed under low pressure N_2 stream flow. The substrates were fixed onto the metallic disc using epoxy glue and transferred to the AFM stage for imaging. Complete AFM analysis of living cells was performed within 2 h after the sample was prepared. Sample preparation and imaging were performed under similar conditions to avoid discrepancies.

Results and Discussions

Assessment of the Growth of Arthrobacter *Strains*

Evaluation of bacteria- uranium (VI) interactions requires knowledge of the growth profile and tolerance to uranium of the individual bacterial strains obtained from the SMCC. The nature of bacteria to multiply its numbers in an exponential growth pattern makes it very important to quantify their growth rate in response to changes in environmental conditions. The 5% PYTG media used in our experiments provided the bacteria with all necessary nutrients for growth and metabolism, creating ideal growth conditions to study any particular phenomena using a cultivation-based time-dependent approach. The increase in cell density calculated over a period of 7 days confirmed the typical exponential growth pattern for bacteria (Figure 1A). When comparing results for cell growth of the different strains over the same period, the hemocytometer counts of the cells showed similar growth patterns and significant differences between the three *Arthrobacter* strains on day 7 ($P < 0.001$, power $= 1$); although the growth of strain G975 slightly overshadowed that of the G968 and G954 strains (Figure 1B).

Assessment of the Resistance of Arthrobacter *Strains to Uranium (VI)*

Wet chemistry, microscopic, and microbiological methods were used to elucidate the resistance mechanisms of three *Arthrobacter* isolates to U(VI), investigate time-dependent

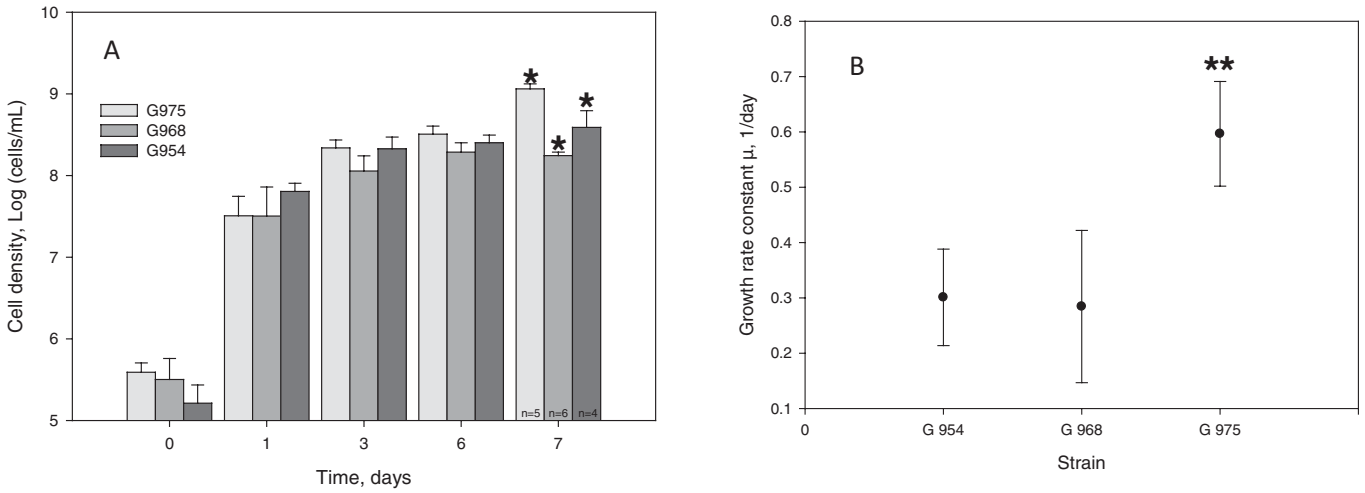

* Statistical significance (P < 0.001, power = 1)

** Statistical significance (P = 0.004, power = 0.973)

Fig. 1. Growth of *Arthrobacter* strains G968, G975, and G954 over 7 days in HEPES-buffered 5% PYTG. A) Log cell concentration over time, n ≥ 4; B) Maximum growth rate constant for each strain, n ≥ 4.

changes in viable cell numbers, and determine the highest concentration of uranium they are able to tolerate and remain viable.

Cell viability in control media without U(VI), determined via colony forming units, ranging at the beginning of the experiment from 4.7–4.8 log CFU/mL, yielded similar CFU counts for all strains over 7 days of cultivation; 7.31–7.38 log CFU/mL was determined for G954 and G968, which was slightly overshadowed by the value of 7.89 log CFU/mL for G975. The mean population density for the same period was changed from 5.6 log cells/mL to 8.6 log cells/mL; a similar pattern was observed for the calculated CFU. The addition of U(VI) to the cultivation media highly inhibited cell viability and CFU counts exhibited a drastic decrease; however, strain tolerance has been shown to vary.

Little to no growth was noted for G968 and G954 by streaking onto petri dishes from cultures amended with 9.5 ppm and 14 ppm of U(VI). G954 showed a significant decline in cell viability in cultures treated with 5 ppm of U(VI). The number of viable cells on the third day was decreased compared to the initial value by 58.6%, and no viable cells were detected by day 7. In contrast, G968 remained viable in the presence of 0.5 ppm of U(VI) and by day 7, the number of viable colonies was comparable to the control without U(VI) (Figure 2).

Of the three strains tested, G975 exhibited the highest tolerance towards U(VI) relative to the other strains and remained viable in the presence of 9.5–19 ppm of U(VI) over the study period. The cell density and CFU counts of viable colonies were increased to values comparable to the control without uranium. G975 was capable of tolerating up to 38 ppm U(VI); however, the number of viable cells gradually declined from initial log 4 cfu/mL to 0 over 6 days (Figure 2). A decline in growth was observed for cultures amended with 48–57 ppm of U(VI), and no viable colonies were detected on day 3. The decrease in CFU counts did not appear to be due to cell lysis, as the initial cell density determined by direct microscopy remained unchanged over the study period (Figure 3).

Experiments with G968 in the media amended with 9.5–14 ppm of U(VI) were repeated with the smaller initial concentration of 1.E+05cells/mL (5 log cells/mL). No viable cells were found on the next day after starting the experiment (data not shown) compare to previous conditions with initial 1.E+06 cells/mL when the number of viable cells for the same period were observed between 1–2.5 log cells/mL. Thus, the cell viability is dependent on the initial concentration of cells. This finding is compatible with the results of (Tsuruta 2002), who found that the relative amount of uranyl ion adsorbed per cell was decreased with increasing cell density, and hypothesized that the lower relative concentrations of U could enhance cellular survival in the presence of toxic substances.

After U(VI) exposure, the colonies on the plates were small in diameter, uniformly circular, entire, and smooth on the agar surface. All strains exhibited presence of a rod-coccus growth cycle. The G975 colonies were golden, and both G968 and G954 were glossy white in color. Control samples cultured on solid glucose media without dilution formed large areas of clusters with CFUs not able to be counted. All of these morphological properties are consistent with those described for the genus *Arthrobacter* (Crocker et al. 2000).

PTYG media components are readily degradable by microorganisms, and measurements of centrifuged supernatant solutions of control tubes inoculated with *Arthrobacter* strains, by day 7, showed a decrease in the TOC content. The initial TOC value of 1014 ± 56 mg/L was reduced by 25%–40.7% for three strains; however, in the presence of U(VI), the TOC degradation was less. G954 treated with 0.5 ppm of U(VI) exhibited 24.7% TOC reduction compared to the 39.8% in control. In contrast, with the increase of U(VI) concentration up to 5ppm, substantial inhibition was observed resulting in only 8.3% reduction in TOC value.

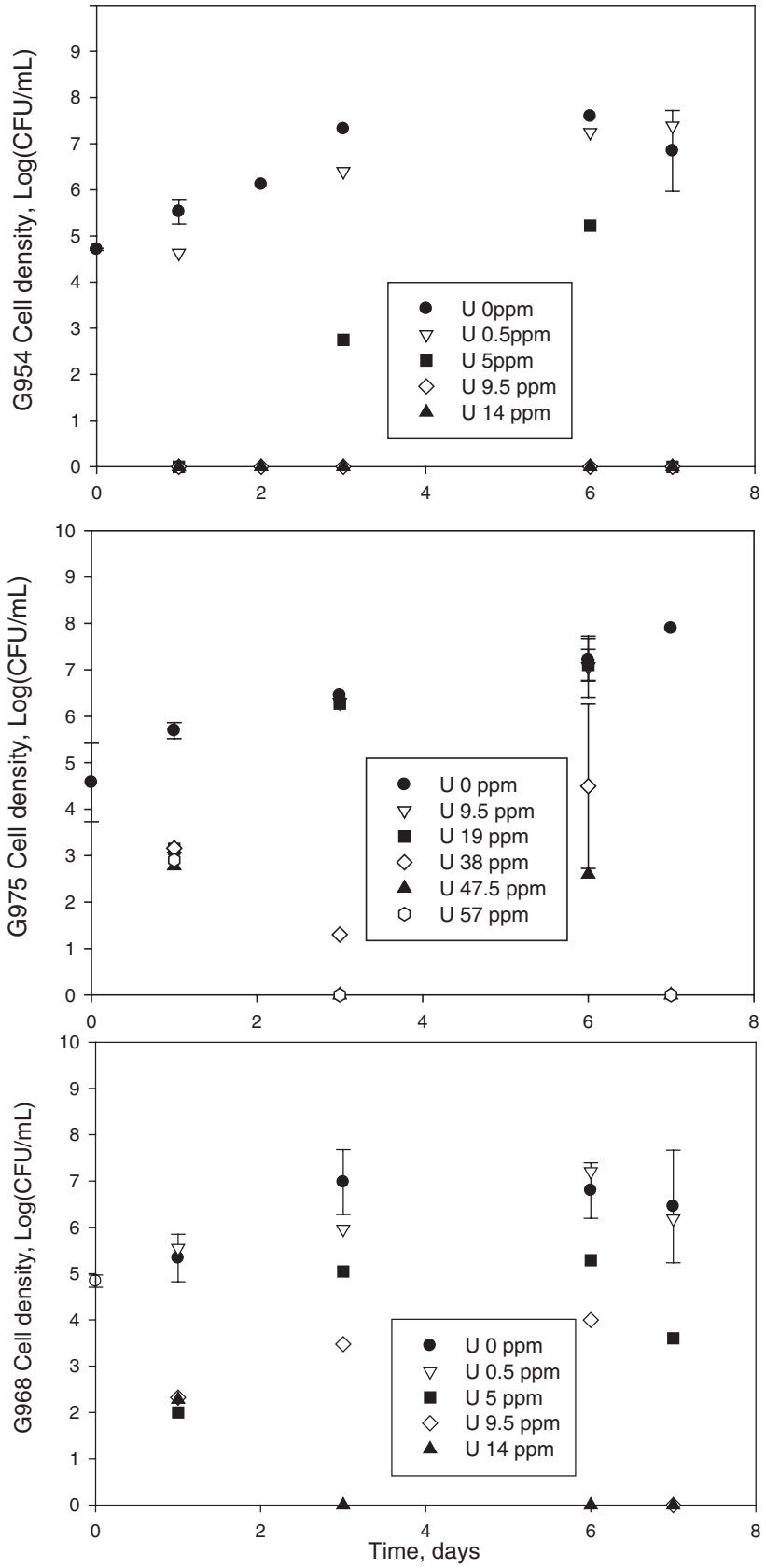

Fig. 2. Changes in colony forming units over a 7-day period in the presence of U(VI), n = 2.

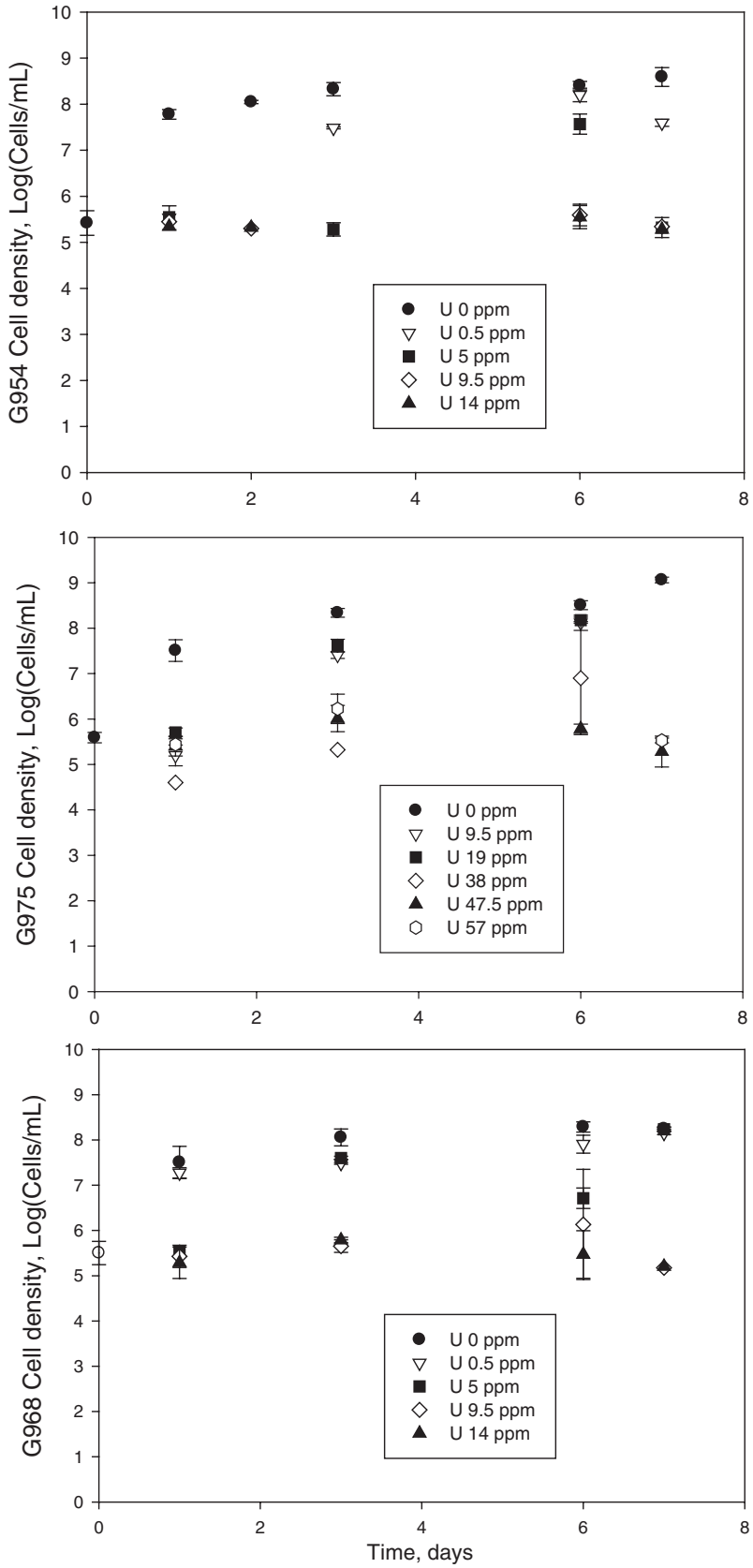

Fig. 3. Changes in cells density over a 7-day period in the presence of U(VI), n = 3.

G968 treated with 0.5 ppm of U(VI) exhibited slightly less reduction in TOC, 23.4% vs. 25% in abiotic control; the inhibition of TOC degradation was noted at 5 ppm of U(VI) with barely 11.6% reduction in TOC value. G975 degraded TOC in the range of 30.7–34.7% after the addition of 9.5–27 ppm of U(VI); but the addition of 38 ppm of U(VI) inhibited the organic carbon consumption to 16.95%, and it remained as low as 4.8% in the presence of 48 ppm. These results revealed that the cell metabolism was altered by uranium, but the inhibitory effect was concentration-dependent for each strain. Triggered by the addition of U(VI) to the media, a decrease in TOC consumption was found for each strain consistent with the loss in cell viability (Figures 2 and 3).

Electron Microscopy

SEM bservations of the bacterial surfaces following uranium tolerance studies indicated that bacterial cells growing in PTYG media were plump and had smooth surfaces. However, as indicated on SEM micrographs, surface of uranium-loaded cells looked distorted and damaged (Figure 4). The alteration in surface morphology for G968 was noted at 0.5 ppm (Figure 4B); G975 shows signs of cell inhibition at the much higher concentration of 19 ppm of (UVI) (Figure 4D).

Incubation of G975 with 27 ppm of U(VI) caused even more distortions for bacterial surface and in addition, a formation of fine precipitate was observed within a bacterial pellet (data

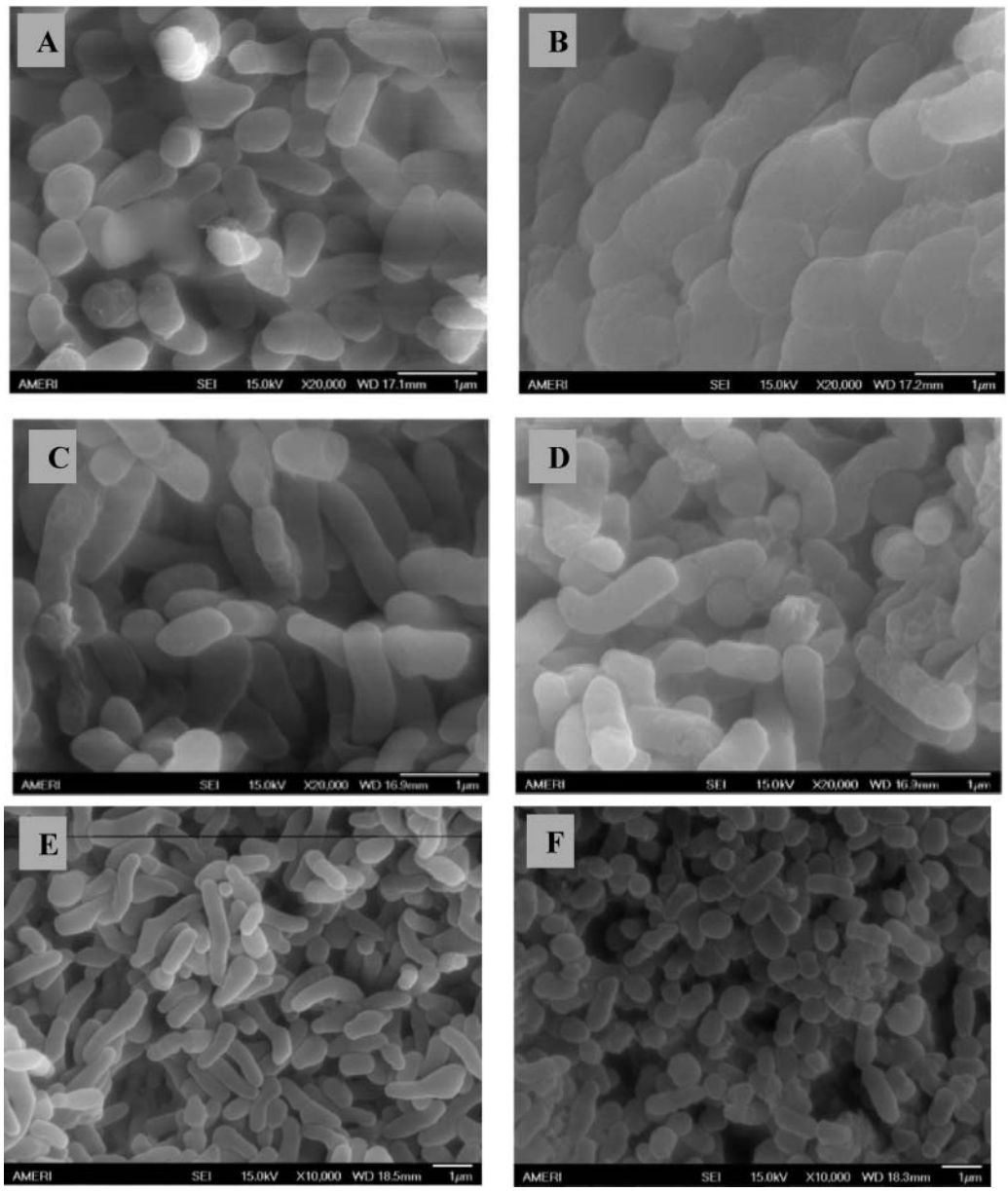

Fig. 4. SEM images: A) G968 U-free control; B) G968 after growing in 0.5 ppm U(VI)-loaded media; C) G975 after growing in 9.5 ppm U(VI)-loaded media; D) G975 after growing in 19 ppm of U(VI)-loaded media; E) G954 after growing in 0.5 ppm of U(VI)-loaded media; F) G954 after growing in 5 ppm of U(VI)-loaded media.

Table 1. Elemental analysis of bacterial surface composition

Strain	U (VI), ppm	Weight,%						Average U uptake,%
		O	Na	Si	P	K	U	
G975	Control	15.29 ± 2.7	0.8 ± 0.02	1.93 ± 0.3	0.43 ± 0.1	—	—	
G975	9.5	11.96 ± 2.6	1.22 ± 0.1	0.66 ± 0.08	1.18 ± 0.2	—	0.52 ± 0.3	90.9 ± 5.8
G975	19	10.27 ± 1.9	1.44 ± 0.1	0.54 ± 0.08	1.66 ± 0.6	—	2.51 ± 0.7	91.29 ± 7.8
G975	27	12.38 ± 0.8	1.93 ± 0.3	0.47 ± 0.1	0.6 ± 0.7	—	2.82 ± 0.8	92.4 ± 4.7
G968	Control	9.48 ± 1.2	1.1 ± 0.07	0.52 ± 0.1	0.41 ± 0.2	0.87 ± 0.12	—	—
G968	0.5	9.5 ± 1.5	0.9 ± 0.08	1.47 ± 0.3	0.59 ± 0.3	0.07 ± 0.05	1.23 ± 0.1	24.6 ± 3.6
G968	5	10.62 ± 4.5	0.3 ± 0.08	0.96 ± 0.5	—	0.05 ± 0.1	1.46 ± 0.5	2.75 ± 0.9
G954	Control	13.28 ± 1.3	2.24 ± 0.2	2.39 ± 0.3	—	—	—	
G954	0.5	14.82 ± 1.7	1.9 ± 0.2	2.4 ± 1.4	—	0.1 ± 0.1	0.16 ± 0.3	34.2 ± 15.5
G954	5	13.06 ± 2.2	0.3 ± 0.1	2.83 ± 0.4	—	0.11 ± 0.04	4.88 ± 1.3	7.43 ± 6.2

not shown). This was attributed to the complex formation between uranium and phosphorus media ingredients that possess high binding affinity for uranium. Preliminary testing on phosphorus content in three PTYG media components such as yeast extract, peptone, and trypton revealed a rather high concentration in yeast extract (1.1%), followed by a negligible amount in peptone; phosphorus was not detected in trypton solution.

Phosphorus in the yeast extract is mostly present in the organic form (Jayasinghearachchi and Seneviratne 2006); however, the release of phosphorus from yeast extract could complex uranium forming uranyl-phosphate solids in the media. Testing of abiotic controls showed some decline in U(VI) concentrations. The results indicated that over a 7-day period the uranium concentration in abiotic control amended up to 30 ppm of U(VI) deviated no more than 6.9 ± 2.6% of its initial value.

At the same higher U(VI) concentrations, SEM analysis of the samples containing microbial culture showed the formation of a precipitate in the experimental media. Perhaps, the complexation of uranium with phosphorus released from yeast extract and formation of uranyl solids aids in reduction of U(VI) toxic effects on the bacteria. This could explain the lag in time which the cells incubated with uranium require to recover before exhibiting some growth, as seen with G975 growing in media amended with 27 ppm of U(VI) (Figures 2 and 3).

Similar changes in surface morphology were observed for G954. The addition of 0.5 ppm of U(VI) did not show a toxic effect on the G954 strain (Figure 4E), but incubation with 5 ppm caused changes in cell morphology resulting in decrease in cell size and distorted surfaces (Figure 4F).

The cell wall of Gram-positive bacteria is made up of a highly cross-linked polymer pepridoglycan rich in carboxylic and phosphate groups (Frankel and Bazylinski 2003). The EDS spectrum of the cell surface confirmed the elemental composition of uranium precipitates comprised mainly of uranium, oxygen, phosphorus, silica, sodium and potassium. Phosphorus was found on the surface of G975 and G968, but was not detected on the surface of the G954 control and cells growing in uranium-amended media. The weight percentage of phosphorus on the cell surface was found to increase when growth media was amplified with a higher concentration of uranium.

Previous studies have shown that bacteria create a very efficient phosphatase-mediated mechanism to activate secretion of phosphate groups. In fact, they can produce excess orthophosphate, protecting cells from the toxic effects of radionuclides via passive U(VI) complexation by the negatively charged cell wall extracellular polymers (Beazley et al. 2007; Macaskie et al. 1994; Martinez et al. 2007; Renninger et al. 2004). Potassium was detected on the surface of G968 and G954 incubated with 0.5 ppm and 5 ppm of U(VI), but not observed on G975, exposed to the same concentrations. The exposure of G975 to U(VI) caused a corresponding increase in Na content on the G975 cell surface, but values for the Na content were down for G954 and G968 (Table 1).

The results of studies demonstrated that the U bioaccumulation was species-specific. Measurements of total soluble uranium showed that the G975 strain exhibited a high uranium accumulating ability. A significant amount of U(VI) ranging from 90.9% to 92.4% was removed by the end of the 7 days of incubation in the studied U(VI) concentrations range up to 27 ppm (Table 1). In contrast, for G968, the amount of uranium taken up by cells for 0.5 ppm was found to be 24.6%, and this value was decreased to 2.75% when growth media was amended with 5 ppm of U(VI). The surface concentrations of Na and K on G968 cells incubated without U(VI) were observed to decrease compared to the control (Table 1).

Reduction in Na weight (%) correlated with the corresponding increase in U(VI) on the cell surface, suggesting that the surface adsorption via an ion exchange is possibly a prevailing mechanism for G968. A similar mechanism can explain U(VI) bioaccumulation on G954 with corresponding measured values of 44.28% and 7.43% for the removal of 0.5 ppm and 5 ppm of uranium relative to abiotic controls. In addition, assessment of bacterial samples after growing in media amended with various concentrations of U(VI), indicated that higher U(VI) weight percentage found on the bacterial cell surface correlated with higher concentrations of uranium added to the culture broth (Table 1).

AFM scans specified cell surface localized precipitation of uranium. From the phase images in Figure 5 (image on the left represents the height data [Z range 250 nm] and on the

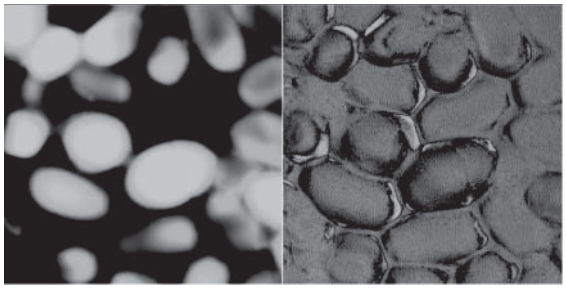

Figure 5 A. G968 control sample (scan size 4.89 × 4.89 μm^2). Phase image clearly shows no precipitation on the cell surface.

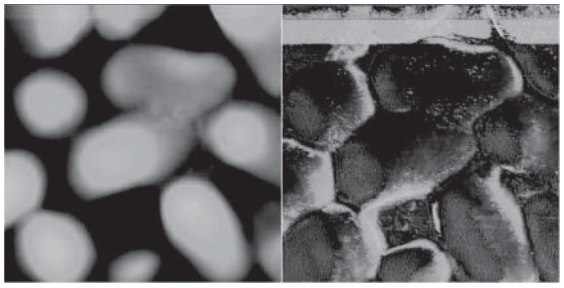

Figure 5B. G968 cultured in the media amended with 0.5ppm of U(VI) (scan size 3.25 × 3.25 μm^2). Phase image clearly shows crystalline deposits on the cell surface, which can also be visualized in height image.

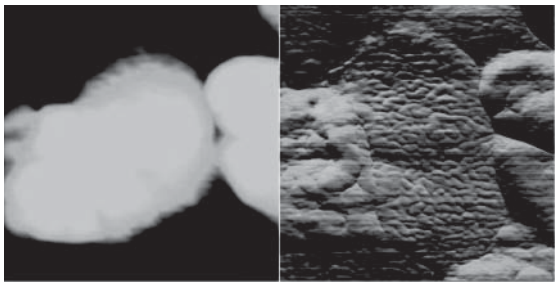

Figure 5C. G975 control sample (scan size 2.94 × 2.94 μm^2) showing its unusual wrinkled surface morphology. The topagraphy image on the left (Z range 200 nm) and frictional image (0.3 V) on the right.

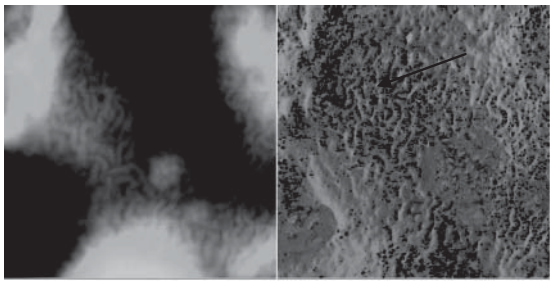

Figure 5D G975 cultured in the media amended with 5ppm uranium (scan size 1.45 × 1.45 μm^2; phase angle 60º). Phase image clearly shows crystalline deposition on the cell surface.

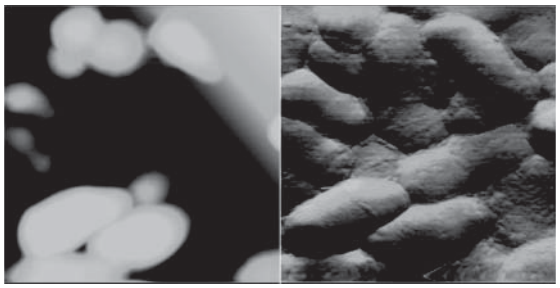

Figure 5E. G954 control sample (scan size 4.77 × 4.77 μm^2; Z range 200 nm and frictional image (0.3 V).

Figure 5F. G954 cultured in the media containing 0.5ppm uranium (scan size 3.89 × 3.89 μm^2; Z range 250nm and phase angle 60º). Height and phase images clearly show precipitation on the cell surface.

Fig. 5. AFM images for morphological comparisons of *Arthrobacter* strains cell-surface accumulation of uranyl after growing in U(VI) amended media (left: the topography image; right: phase image).

right represents the phase data [phase angle 60°]), uranium precipitates deposited on the cell surface are distinctly visualized as clearly defined crystalline deposits on the cell surface of uranium treated samples, while the surface topographic features of the control samples show no precipitation. The experimental results suggest that G975 is a uranium-resistant *Arthrobacter* strain with the superior ability to tolerate higher concentrations of U(VI).

Additionally, this strain accumulated up to 92% of uranium in the studied U(VI) concentrations range up to 27 ppm, which is almost triple the value compared to the G968 and G954 strains (Table 1). This high uranium uptake can be attributed to several factors: the ability to produce excess phosphorus correlated with a corresponding increase in U(VI) concentration in growth media and the highly irregular cell surface structure, which provides larger surface area for uranium precipitation spread over the entire cell as fine-grained, platy uranium minerals (Figure 5C, Figure 5D). A similar accumulation was reported for surface-bound uranium in *Bacillus sphaericus JG-A12* implicated due to physical and chemical interactions with specific carboxyl and phosphate functional groups situated on the cell surface (Merroun et al. 2005).

AFM images of G954 living cells have shown surface precipitation of uranium (Figure 5F); however, EDS spectra of the cell surface have not confirmed the presence of phosphorus in the elemental composition of control samples and

ones cultured in the media amended with uranium. It might be that cell surface composition was altered during fixation for SEM/EDS analysis. Precipitated uranium-bearing crystals on the bacterial surface of G968 and G975, as observed at SEM/EDS analysis, were composed of U and P.

Previous research (Martinez et al. 2007; Nedelkova et al. 2007; Suzuki and Banfield 2004) identified bacterial uranium precipitation as autunite/meta-autunite mineral phases at pH ranging from 4.5 to 7. Macaskie et al. (1992, 1994) observed precipitation around the cells of *Citrobacter* sp. composed of HUO_2PO_4 and $NaUO_2PO_4$ at pH 6.9. Precipitation of uranium on the outer cell wall surface functions as a protection mechanism to uranium toxicity; however, cell-surface mineralization, which is increased upon addition of higher uranium concentrations, may result in inhibition of membrane metabolic functions and disruption of nutrient transport resulted in the decreased viability.

This finding agrees with previous research, suggesting that the binding of uranyl to the cell envelope and cell surface-associated mineralization result in the inhibitory effect on metabolism, which includes limitation of nutrient transport and disruption of the proton motive forces (Bencheikh-Latmani and Leckie 2003; Southam 2000). At neutral pH, the data of thermodynamic speciation modeling indicates the predominance of hydroxo uranium species such as $(UO_2)_3(OH)_5^+$, UO_2OH^+, and $(UO_2)_4(OH)_7^+$ in aqueous media solution. These species are cations and most likely to be considered as possible inhibitors due to binding to negatively charged bacterial cell surfaces.

Conclusions

Interactions amongst radionuclides and microbes are important factors affecting metal mobility in the subsurface. At sites where the concentration of metal contaminants can reach toxic levels, the metal resistances of indigenous microbial populations serve as a critical parameter for the success of *in situ* remediation efforts. Assessment of the uranium resistance of *Arthrobacter* sp. has been carried out by culturing the bacterial cells in various concentrations of uranium (VI) (0.5–57 ppm). The cell density and viability data has shown that G975 is the fastest growing and the most uranium-tolerant strain, with abilities to survive in the presence of up to 38 ppm of U(VI).

The results of this study demonstrated that due to its unique irregular surface structure, this strain can accumulate more than 90% of uranium. No significant difference in the cell growth rate constant was observed between the G954 and G968 strains ($P = 0.82$), and similar ion exchange and uranium surface precipitation mechanisms can explain U(VI) uptake for both strains. The cell metabolism was altered by uranium, but the inhibitory effect was concentration dependent for each strain. SEM/EDS indicated surface morphological changes and signs of cell inhibition in the presence of uranium. The EDS spectrum of the cell surface confirmed the elemental composition of uranium precipitates and revealed the uranium adsorbance on bacterial surfaces. Microbial precipitation of uranium on bacterial surfaces may offer a solution to sequester uranium in aerobic environments such as the vadose zone.

References

Araujo JC, Téran FC, Oliveira RA, Nour EAA, Montenegro MAP, Campos JR, Vazoller RF. 2003. Comparison of hexamethyldisilazane and critical point drying treatments for SEM analysis of anaerobic biofilms and granular sludge. J Electron Microsc 52(4):429–433.

Balkwill DL, Reeves RH, Drake GR, Reeves JY, Crocker FH, King MB, Boone DR. 1997. Phylogenetic characterization of bacteria in the subsurface microbial culture collection. FEMS Microbiol Rev 20:201–216.

Beazley MJ, Martinez RJ, Sobecky PA, Webb SM, Taillefert M. 2007. Uranium biomineralization as a result of bacterial phosphatase activity: Insights from bacterial isolates from a contaminated subsurface. Environ Sci Technol 4:5701–5707.

Bencheikh-Latmani R, Leckie JO. 2003. Association of uranyl with the cell wall of *Pseudomonas fluorescens* inhibits metabolism. Geochim Cosmochim Acta 67(21):4057–4066.

Boylen CW. 1973. Survival of *Arthrobacter crystallopoietes* during prolonged periods of extreme desiccation. J Bacteriol 113:33–37.

Burns PC. 1999. The crystal chemistry of uranium. Rev Mineral Geochem 38:23–90.

Crocker FH, Fredrickson JK, White DC, Ringelberg DB, Balkwill DL. 2000. Phylogenetic and physiological diversity of *Arthrobacter* strains isolated from unconsolidated subsurface sediments. Microbiology 146:1295–1310.

Davis JA. 2001. Surface complexation modeling of uranium (VI) adsorption on natural mineral assemblages. Report NUREG/CR- 6708. Rockville, MD: U.S. Nuclear Regulatory Commission.

Finch RJ, Murakami T. 1999. Systematics and paragenesis of uranium minerals. In: Burns PC, Finch R, editors, Uranium: mineralogy, geochemistry and the environment. Reviews in Mineralogy. Washington, DC: Mineralogical Society of America, vol. 38; p91–179.

Francis AJ. 2008. Microbial Transformations of Uranium in Wastes and Implication on its Mobility. Proceedings of the International Conference on Uranium Mining and Hydrogeology; Freiberg, Germany. UMH V TU Bergakademie. p14–18.

Francis AJ, Gillow JB, Dodge CJ, Harris R, Beveridge TJ, Papenguth HW. 2004. Association of uranium with halophilic and nonhalophilic bacteria and archaea. Radiochim Acta 92:481–488.

Frankel RB, Bazylinski DA. 2003. Biologically induced mineralization by bacteria. Rev Mineral Geochem 54:95–114.

Fratesi SE, Lynch FL, Kirkland BL, Brown LR. 2004. Effects of SEM preparation techniques on the appearance of bacteria and biofilms in the carter sandstone. J Sediment Res 74(6):858–867.

Fredrickson JK, Zachara JM, Balkwill DL, Kennedy D, Li SW, Kostandarithes HM, Daly MJ, Romine MF, Brockman FJ. 2004. Geomicrobiology of high-level nuclear waste-contaminated vadose sediments at the Hanford Site, Washington State. Appl Environ Microbiol 70(7):4230–4241.

Grenthe I, Fuger J, Konings RJM, Lemire RJ, Muller AB, Nguyen-Trung C, Wanner H. 2004. The Chemical Thermodynamics of Uranium. New York: Elsevier.

Guillaumont R, Fanghanel T, Fuger J, Grenthe I, Neck V, Palmer DA, Rand MH. 2003. Chemical Thermodynamics 5. Update on the Chemical Thermodynamics of Uranium, Neptunium, Plutonium, Americium and Technetium. Amsterdam: Elsevier.

Jayasinghearachchi HS, Seneviratne G. 2006. Fungal solubilization of rock phosphate is enhanced by forming fungal–rhizobial biofilms. Soil Biol Biochem 38(2):405–408.

Kieft TL. 2002. Hot desert soil communities. In: Bitton G, editor. Encyclopedia of Environmental Microbiology. New York: John Wiley. p1576–1586.

Lenhart JJ, Cabaniss SE, MacCarthy P, Honeyman BD. 2000. Uranium(VI) complexation with citric, humic and fulvic acids. Radiochim Acta 88:345–353.

Macaskie LE, Bonthrone KM, Rouch DA. 1994. Phosphatase mediated heavy metal accumulation by a *Citrobacter* sp. and related enterobacteria. FEMS Microbiol Lett 121:141–146.

Macaskie LE, Empson RM, Cheetham AK, Grey CP, Skarnulis AJ. 1992. Uranium bioaccumulation by a *Citrobacter* sp. as a result of enzymically mediated growth of polycrystalline HUO_2PO_4. Science 257:782–784.

Martinez RJM, Beazley J, Teillefert M, Arakaki AK, Skolnick J, Sobecky PA. 2007. Aerobic uranium (VI) bioprecipitation by metal-resistant bacteria isolated from radionuclide- and metal-contaminated subsurface soils. Environ Microbiol 9:3122–3133.

Merroun ML, Raff J, Rossberg A, Hennig C, Reich T, Selenska-Pobell S. 2005. Complexation of uranium by cells and S-layer sheets of *Bacillus sphaericus* JG-A12. Appl Environ Microbiol 71(9):5532–5543.

Mongodin EF, Shapir N, Daugherty SC, DeBoy RT, Emerson JB, Shvartzbeyn A, Radune D, Vamathevan J, Riggs F, Grinberg V, Khouri H, Wackett LP, Nelson KE, Sadowsky MJ. 2006. Secrets of soil survival revealed by the genome sequence of *Arthrobacter aurescens* TC1. PLoS Genet 2(12):e214.

Nedelkova M, Merroun ML, Rossberg A, Hennig C, Selenska-Pobell S. 2007. Microbacterium isolates from the vicinity of a radioactive waste depository and their interactions with uranium. MS Microbiol Ecol 59:694–705.

Osman S, Peeters Z, La Duc MT, Mancinelli R, Ehrenfreund P, Venkateswaran K. 2008. Effect of shadowing on survival of bacteria under conditions simulating the Martian atmosphere and UV radiation. Appl Environ Microbiol 74(4):959–970.

Renninger N, Knopp R, Nitsche H, Clark D, Keasling J. 2004. Uranyl precipitation by *Pseudomonas aeruginosa* via controlled polyphosphate metabolism. Appl Environ Microbiol 70:7404–7412.

Southam G. 2000. Bacterial surface-mediated mineral formation. In Lovley DR, editor. *Environmental Microbe–Metal Interactions*. Washington, DC: ASM Press. p. 257–276.

Suzuki Y, Banfield JF. 2004. Resistance to, and accumulation of, uranium by bacteria from a uranium-contaminated site. Geomicrobiol J 21:113–121.

Tsuruta T. 2002. Removal and recovery of uranyl ion using various microorganisms. J Biosci Bioeng 94:23–28.

Van Waasbergen LG, Balkwill DL, Crocker FH, Bjornstad BN, and Miller RV. 2000. Genetic Diversity among *Arthrobacter* species collected across a heterogeneous series of terrestrial deep-subsurface sediments as determined on the basis of 16S rRNA and recA gene sequences. Appl Environ Microbiol 66(8):3454–3463.

Zachara J, Brown C, Christensen J, Liu C, Davis J, Dresel E, Kelly S, Liu C, McKinley J, Serne J, Um W. 2007. A site-wide perspective on uranium geochemistry at the Hanford Site. PNNL-17031 report written for CH2M HILL Hanford Group, Inc. Available at http://water.usgs.gov/nrp/proj.bib/Publications/2007/zachara_liu_etal_2007.pdf